

Review

Immobilized Nanomaterials for Environmental Applications

Francisco J. Cervantes * and Luis A. Ramírez-Montoya 

Laboratory for Research on Advanced Processes for Water Treatment, Engineering Institute, Campus Juriquilla, Universidad Nacional Autónoma de México (UNAM), Blvd. Juriquilla 3001, Querétaro 76230, Mexico

* Correspondence: fcervantesc@iingen.unam.mx

Abstract: Nanomaterials (NMs) have been extensively used in several environmental applications; however, their widespread dissemination at full scale is hindered by difficulties keeping them active in engineered systems. Thus, several strategies to immobilize NMs for their environmental utilization have been established and are described in the present review, emphasizing their role in the production of renewable energies, the removal of priority pollutants, as well as greenhouse gases, from industrial streams, by both biological and physicochemical processes. The challenges to optimize the application of immobilized NMs and the relevant research topics to consider in future research are also presented to encourage the scientific community to respond to current needs.

Keywords: biodegradation; bioenergy production; greenhouse gases; industrial wastewater treatment; recalcitrant contaminants

1. Introduction

The superior catalytic properties of nanomaterials (NMs) as compared to their bulk precursors have encouraged their application in several fields, including for environmental purposes, such as the removal of persistent contaminants, stimulation of microbial processes for bioenergy production, and reduction of greenhouse gas (GHG) emissions [1,2]. Nevertheless, NMs cannot be used in suspension in engineered systems since their recovery is expensive and unreasonable in post-treatments in full-scale operations. Furthermore, the discharge of NMs to environmental reservoirs represents a serious risk, and their use in engineered systems could be counterproductive, since many of these manufactured materials may have environmental and public health consequences, such as genotoxicity and cytotoxicity [3]. Accordingly, strategies to immobilize NMs in treatment systems for several distinct applications have been developed. These immobilizing techniques are particularly relevant for environmental purposes. Among the main advantages related to the use of immobilized NMs as catalysts are: (1) facile separation and retention of the catalysts in the reaction system; (2) continuous operation proceeds smoothly; and (3) the combined effects of catalysis and adsorption with NMs cover both commitments. Nevertheless, some disadvantages could also arise from the use of immobilized NMs which need to be addressed in future works, such as deactivation, poisoning, or washout of the catalysts, as well as mass-transfer limitations [4]. The purpose of this review is to provide an overview of the main strategies to immobilize NMs for their application in different environmental engineered processes (Figure 1). Particularly, this paper summarizes the application of immobilized NMs in the production of renewable energies, as well as the removal of recalcitrant pollutants and GHGs from industrial discharges.



Citation: Cervantes, F.J.;

Ramírez-Montoya, L.A. Immobilized Nanomaterials for Environmental Applications. *Molecules* **2022**, *27*, 6659. <https://doi.org/10.3390/molecules27196659>

Academic Editor: Luciana Pereira

Received: 8 September 2022

Accepted: 5 October 2022

Published: 7 October 2022

Publisher's Note: MDPI stays neutral with regard to jurisdictional claims in published maps and institutional affiliations.



Copyright: © 2022 by the authors. Licensee MDPI, Basel, Switzerland. This article is an open access article distributed under the terms and conditions of the Creative Commons Attribution (CC BY) license (<https://creativecommons.org/licenses/by/4.0/>).

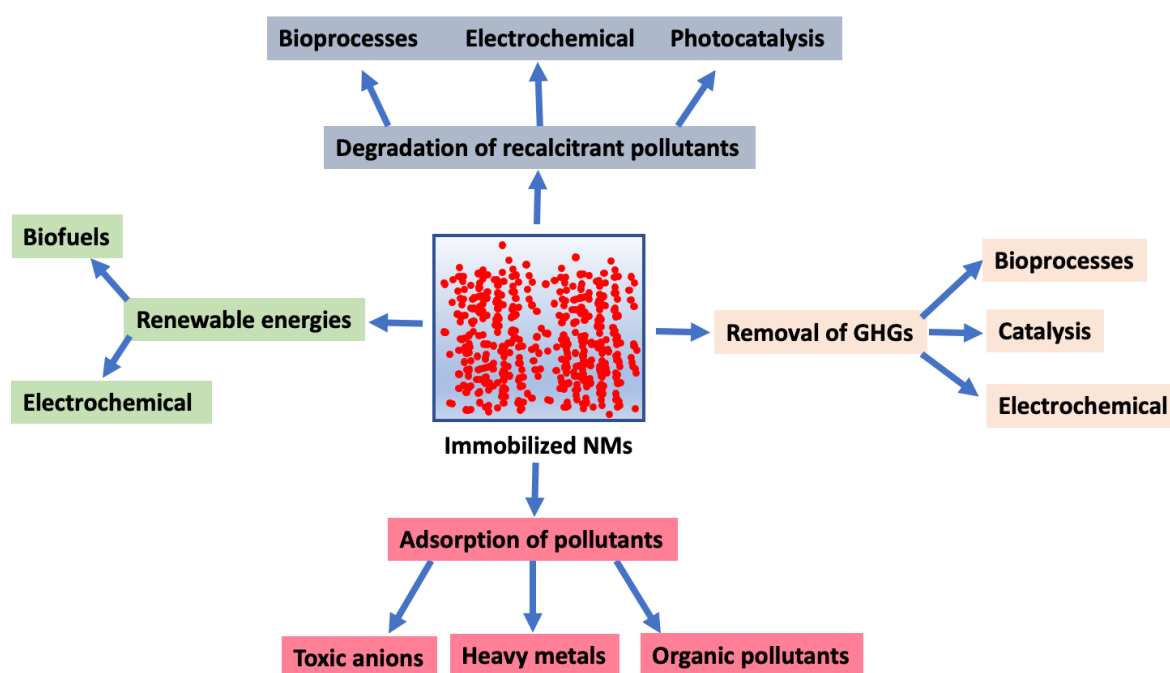


Figure 1. Key environmental applications of immobilized nanomaterials (NMs). GHGs, greenhouse gases.

2. Immobilized NMs for Energy Production

2.1. Biofuels

Global warming caused by anthropogenic emissions associated with the conventional production of fuels has exacerbated the living conditions of our planet, putting at risk the sustainability required for future generations. Consequently, the introduction of renewable energy sources to replace fossil fuels will play a pivotal role in tackling this menace. Methane is a renewable energy source, which can be sustainably obtained in engineered systems during the treatment of industrial wastewaters, as well as solid residues, such as animal manure or the organic fraction of municipal solid waste, by a process denominated anaerobic digestion (AD) [5]. AD comprises a complex route in which several anaerobic microorganisms are responsible for converting organic substrates into biogas under anaerobic conditions. In the last few years, the role of conductive NMs on AD processes has received a lot of attention because their application to anaerobic bioreactors has significantly increased the methane production from synthetic and real wastewaters [5]. NMs applied in these studies include carbon-based materials, such as graphene oxide (GO) and carbon nanotubes (CNT), in addition to metallic NMs, such as magnetite, nano zero-valent iron (nZVI), silver, and different iron oxides [6].

Recently, direct interspecies electron transfer (DIET) has been reported involving the formation of an electric current between electron-donating and electron-accepting microorganisms. For example, DIET has been shown to occur in cocultures of *Geobacter* species and acetoclastic methanogens, such as *Methanosarcina* sp., and this electron-transferring mechanism has been pointed out as one of the reasons for the improved performance of anaerobic bioreactors for producing methane in the presence of conductive materials (CM) [7]. Certainly, it was shown that the lack of pili and other cellular structures involved in electron transfer in microbial consortia can be compensated by the presence of CM [7,8]. Nevertheless, additional studies have indicated that the input of CM on AD processes goes beyond the stimulation of DIET because electric conductivity is not the only relevant parameter [6,9]. In fact, several physical-chemical properties of NMs, such as particle size, functional group, and surface area, drive the interactions between these materials and anaerobic microorganisms, ultimately determining the performance of anaerobic bioreactors during the production of methane from wastewater and solid residues. For instance,

oxidized functional groups in GO promoted strong interaction between this material and anaerobic microorganisms, in a methanogenic consortium, causing the wrapping of cells and, consequently triggering mass-transfer limitations during the conversion of complex substrates, such as starch, which was reflected in a lower production of biogas [10]. However, when GO was applied in its reduced form (GOr) to the same consortium, this CM did not cover the cells and stimulated a greater production of methane [11].

Efforts to apply immobilized NMs to improve the production of methane from wastewater have recently been reported. For instance, nano-magnetite was fixed in granular activated carbon (GAC) for its subsequent application for the anaerobic treatment of low-strength wastewater [12]. The synthesized composite was mixed with anaerobic sludge in a bioreactor, which showed superior conductivity and electron-transferring capacity, ultimately fueling 3.6-fold higher methane production, as compared to the control bioreactor. Interestingly, the application of immobilized nano-magnetite triggered a higher abundance of functional microorganisms. Additionally, a strategy for in situ formation and self-immobilization of biogenic iron oxides in anaerobic granular sludge revealed an effective improvement of the production of methane, which was attributed to increased conductivity and stimulated growth of exoelectrogens (i.e., microorganisms with the capacity to donate electrons, such as *Clostridium*) and endoelectrogens (i.e., microorganisms with the ability to accept electrons, such as *Methanosaeta*) [13]. More recently, GO was immobilized in organic xerogels, which were applied for the treatment of protein-rich wastewater. The addition of this composite promoted higher methane production and the superior removal of organic matter and ammonium, as well as the production of medium chain fatty acids [14].

Hydrogen (H₂) is the only carbon-free fuel available, and is expected to play a crucial role in the future energy market due to its high energy content and clean combustion product [15]. H₂ can also be obtained by anaerobic consortia under more controlled conditions (dark fermentation). Furthermore, several metallic NMs, such as nanoparticles (NPs) of Ag, Au, Ni, and Fe₂O₃, have been shown to enhance H₂ production in terms of production rate, as well as yield [16–19]; thus, it is conceivable that these NMs could also be immobilized and applied in dark fermentation processes for improving the production of this green biofuel. Besides this, the immobilization of *Enterobacter aerogenes* on CNT improved the H₂ production rate and yield as compared to the performance observed with free cells [20].

Magnetic nanoparticles (MNPs) represent another efficient way to keep catalysts immobilized in bioreactors, and has successfully been applied for improving AD processes [6]. Besides this, MNPs have also been extensively explored as a carrier material for immobilizing enzymes linked to biodiesel and bioethanol production [21]. Immobilized microorganisms/enzymes in MNPs can easily be recovered from fermentation broth for subsequent use in several cycles, which significantly decreases the operational costs in biofuel production. For example, immobilized *Saccharomyces cerevisiae* achieved an ethanol productivity of 264 g/L-h from corn starch and was effectively maintained in several cycles for more than a month [22]. Furthermore, cellulase immobilized in MNPs achieved an efficient hydrolysis of *Sesbania aculeate* biomass yielding up to 5.3 g/L of ethanol along with the reuse of the nano-biocatalysts several times [23]. In another study, biodiesel production from microalgal oil was sustained for up to seven regenerations with a yield reaching 94% under optimal conditions [24].

2.2. Electrochemical Energy Applications

Biogenic NPs have been integrated into bio-electrochemical systems, together with different microorganisms to produce biohydrogen or bioelectricity. For instance, Orozco et al. (2010) [25] combined Pd NPs with *E. coli* for the conversion of H₂ into energy in a fuel cell. Similar studies were also reported in bio-electrochemical systems in which Pd or Pt NPs were immobilized, together with cultures of *Pseudomonas putida* [26], *Desulfovibrio desulfuricans* [27], *Shewanella oneidensis* [28], and *Saccharomyces cerevisiae* [29].

Graphene, jointly immobilized with NPs, has also appeared as a stirring material applied in electrochemical systems for energy storage and conversion applications in lithium batteries and supercapacitors, among other power applications [30]. In fact, the manufacturing of composites created with metallic NPs and graphene has allowed us to overcome some limitations during the application of these NMs in lithium batteries (LBs). For example, Co_3S_4 has the potential to be used as anode material in LBs, but shows capacity vanishing, low conductivity, and poor cyclability [31]. In contrast, the deposition of Co_3S_4 nanotubes on graphene allows better cycling performance and greater reversible capacity as compared to the pristine Co_3S_4 electrode [32]. The additional doping of anodes with elements belonging to group IV, such as Ge and Sn, has significantly enhanced Li-storage capacities, conductivity, reversible capacity, coulombic efficiency, and rate capability [30].

Supercapacitors (SCs) are electrochemical power-storage devices, which compile and discharge energy by reversible adsorption and desorption of ions at the boundaries between electrode constituents and electrolytes. Due to its large available surface, graphene represents an attractive material for electrodes in SCs [33]. In addition, the doping of graphene with $\text{Ni}(\text{OH})_2$ NPs resulted in better electrode–electrolyte interaction, enhancing the conductivity of ions and electrons, ultimately resulting in a superior performance of SCs [34].

Further applications of immobilized NMs in electrochemical energy devices include their employment as composite catalysts to convert solar energy into chemical energy by splitting water into hydrogen photocatalytically. Additionally, graphene-based composites have successfully been applied as photocatalysts to reduce CO_2 into reactive carbon forms [30]. Table 1 summarizes the application of immobilized NMs for energy production.

Table 1. Application of immobilized nanomaterials for energy production.

| Immobilized NMs | Application | Achievement | Reference |
|------------------------------------|--|---|-----------|
| Bioprocesses | | | |
| MNPs | Methane production from low-strength wastewater | 3.6-fold higher methane production as compared to the control bioreactor | [12] |
| BIO | Methanogenic process | 42% higher production of methane as compared to control | [13] |
| GO-OX | Methanogenic process | Higher COD and ammonium removal from protein-rich wastewater as compared to control | [14] |
| MNPs | Fermentative production of ethanol | Ethanol productivity of 264 g/L-h from corn starch, maintained in several cycles | [22] |
| MNPs | Fermentative production of ethanol from <i>Sesbania aculeate</i> biomass | Immobilized cellulase produced 5.3 g/L of ethanol along with the reuse of the nano-biocatalysts several times | [23] |
| MNPs | Biodiesel production from algal oil | Yield reaching 94% was maintained several cycles under optimal conditions | [24] |
| Electrochemical processes | | | |
| Pd, Pt | Pd NPs immobilized together with different microorganisms to produce energy in BES | Enhanced production of hydrogen or electricity as compared to controls without NPs | [26–29] |
| Co_3S_4 -graphene | Lithium battery | Better cycling and greater reversible capacity as compared to the pristine Co_3S_4 electrode | [32] |
| $\text{Ni}(\text{OH})_2$ -graphene | Supercapacitor | Better electrode–electrolyte interaction, enhancing the conductivity of ions and electrons, resulting in a higher performance | [34] |
| Graphene-CX | Aqueous supercapacitor | Combination of high porosity and electrical conductivity for 25% more capacitance and 100% more power than undoped CX at high current densities | [35] |
| S-I Pd aerogel | Microfluidic fuel cell | First time microwave-assisted synthesis of Pd aerogels with enhanced power densities for formic acid electro-oxidation | [36] |

BES, bio-electrochemical systems; BIO, biogenic iron oxide; COD, chemical oxygen demand; CX, carbon xerogel; GO-OX, graphene oxide-organic xerogel; MNPs, magnetic nanoparticles; NPs, nanoparticles; S-I, self-immobilized.

3. Immobilized NMs for the Removal of Recalcitrant Contaminants

3.1. Bioprocesses

Recalcitrant pollutants are defined as those in which the chemical structure is very stable and, consequently, are hardly degraded in conventional biological treatment systems. Many of these recalcitrant compounds are found at trace levels in wastewater; yet, due to their high environmental risks associated with human health and ecotoxicology, their removal is a priority [37]. In order to increase the biodegradability of persistent contaminants, distinct nano-catalysts have been applied in bioreactors. Particularly, strategies to immobilize these NMs to enhance the biodegradation of recalcitrant pollutants have recently been reported (Figure 2). For instance, De Corte et al. (2012) [38] proposed several retention mechanisms for applying biogenic nano-palladium (Bio-Pd) in the bioremediation of waters contaminated with chlorinated solvents and pharmaceuticals in different reactor configurations, such as retention by hollow fiber and plate membranes, encapsulation in alginate beads and polymeric membranes, and coating on zeolites. Bio-Pd has also been immobilized in anaerobic granular sludge for its application as a biocatalyst in the anaerobic biotransformation of pharmaceuticals, chlorinated solvents, azo dyes, nitroaromatics, and Cr^{6+} [37,39,40]. Additionally, Bio-Pd has been immobilized in the cathode of a bio-electrochemical reactor, which achieved a removal rate of tri-chloro-ethylene (TCE) of $151 \text{ g/m}^3\text{-d}$. This removal rate allowed 93% removal of TCE in the Pd-doped system, while only 48% removal was observed in the absence of this nano-catalyst [41].

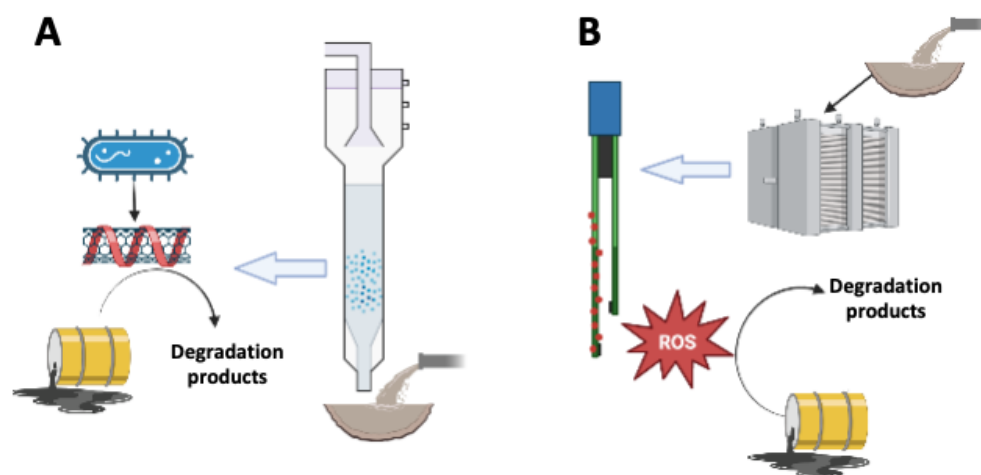


Figure 2. Mechanisms involved in the degradation of recalcitrant pollutants mediated by immobilized NMs in bioprocesses (A) and in electrochemical systems (B). Bacteria reduce conductive NMs (e.g., nanotubes), which promote redox reactions driving the biodegradation of contaminants (A). Immobilized NMs in electrochemical systems produce reactive oxygen species (ROS), which stimulate the degradation of contaminants (B).

Furthermore, graphene-anaerobic sludge composite was shown to be effective for enhancing the rate of reductive biotransformation of nitrobenzene up to twofold [42]. More recently, magnetic graphene oxide nano-sacs (MGONS), immobilized in anaerobic bioreactors, greatly stimulated the biotransformation of iopromide. Indeed, a higher removal efficiency and greater extent of biodegradation occurred in the bioreactor amended with MGONS as compared to the control system lacking this catalyst [43]. NMs have also served as a core for holding redox-active molecules, such as quinones and humic substances, and their application has greatly enhanced the reductive biotransformation of chlorinated solvents and azo dyes [44–46].

Additional applications were reported with microbial cells of *Pseudomonas delafieldii* coated with MNPs, which improved the mass-transfer rate during the desulfurization of dibenzothiophene, which could be relevant for engineered treatment systems in the petrochemical sector [47].

3.2. Electrochemical Systems

Electrochemical technologies, such as electro-oxidation, electro-coagulation, and electro-flotation, have gained attention for the treatment of complex wastewater, disinfection of drinking water, as well as the removal of hazardous, persistent contaminants [48]. Electro-oxidation has emerged as an environmentally friendly process remediation technique, since few or no chemicals are needed to facilitate wastewater treatment, reaching more efficient means, low energy consumption, and convenient operation during wastewater treatment as compared to the biological (aerobic and anaerobic) and physicochemical (membrane technologies, adsorption, and ozonation) alternatives [49]. Electro-oxidation involves the production of strong oxidants (particularly hydroxyl radicals) during the treatment in situ, either directly at the electrode or indirectly from chemical compounds in the treated water [50]. Among the advanced oxidation processes (AOPs), electro-Fenton is an effective method to degrade refractory organic compounds, including dyes, phenol compounds, oil-refining wastewater, and pharmaceutical compounds [51–53]. However, several drawbacks, such as particle agglomeration, low recyclability, and high dependence on the main electrode, still exist, hindering its application [54]. The use of heterogenous nanocomposites appears an alternative to overcome these disadvantages, since the development of stable, inexpensive, selective, and high-performing electrocatalysts is imperative to scaling up this technology to industrial levels. Recently, the immobilization of bimetallic NPs (Ni/Co) on metal organic frameworks (MOF), based on nitrogen-doped porous carbon rods, was carried out for the development of an efficient heterogenous electro-Fenton catalyst and successfully used in the degradation of organic compounds, including tetracycline, chloramphenicol, ciprofloxacin, diclofenac sodium, and sulfamethoxazole, due to reactive oxygen species (ROS) driving the reactions [55]. MOF were also used for the encapsulation of Fe₃O₄ NPs, showing an enhanced degradation of heterocycles, phenols, and esters in old landfill leachate [56]. Changes in the electrode are also reported for the electro-oxidation of diclofenac by the tailoring of a Cu-GOR electrode with a high oxidative current response and high removal efficiencies [57]. Moreover, the electrocatalytic degradation of methyl orange was accomplished using nano-Fe₃O₄ supported on carbon black, which was used as electrode [49].

3.3. Photocatalytic Applications

Photocatalytic degradation of recalcitrant pollutants, using nano-catalysts, has gained attention due to its efficiency, cost effectiveness, low toxicity, low harmfulness, high durability, super-hydrophilicity, photochemical and chemical stability features, and eco-friendly status, leading to complete mineralization and the overcoming of the drawbacks of traditional techniques [58]. The entire mineralization of organic compounds is reached when a semiconductor is irradiated with some light source promoting the formation of valence band holes due to electron excitation, where reactive oxygen species are produced [59]. Photocatalysis is a type of AOP that relies on hydroxyl-radical generation, based on the interaction of a photocatalyst with the incident light energy. This technology is very mature and there are several reviews about its use [60,61], with an estimate of 48,000 publications about dye photocatalytic degradation only under UV and visible light irradiation [62]. Recent trends have led to the development of nano-photocatalysis, since the advantages of NMs result in greater photocatalytic activity and complete mineralization of some pollutants into simple compounds. In nano-catalysis, the movement of electrons and holes, which is crucial for the application of photocatalysis, is also affected by the size and configuration of the NMs.

However, nano-catalysts need to be immobilized in organic/inorganic matrixes to allow liquid–solid separation and recycling efficiency for an effective degradation process [63]. Several photocatalysts have been used for environmental applications (TiO₂, ZnO, WO₃, CuS, SnO₂, CdS, etc.), but most of these photocatalysts are only active under UV light because of a comparatively large bandgap. In terms of supporting materials, the most commonly used include glass, stainless steel, plastics, textiles, alumina, silica, and titania [64].

Recent works in this area are focused on the generation of low-cost nanocatalysts using wasted and recyclable materials as carriers for applications in the removal of different target contaminants, such as dyes, pharmaceutical compounds, and heavy metals [65]. Materials such as polyethylene terephthalic (PET), polystyrene (PS), disposal textile fabrics, newspapers, aluminum soda cans, rubber, waste electronic and electric components and used batteries have been employed as supports for immobilizing catalysts [65]. The use of these carriers represents an eco-friendly alternative for photocatalytic purposes. For instance, the use of wasted silicon powder for the immobilization of synthetic La/TiO₂ NPs significantly improved the degradation of dimethyl phthalate [66]. Additionally, the potential of chitosan-conjugated manganese to produce a magnetic nano bio-composite for the treatment of emerging dye pollutants [58], and harnessing solar light using nano-ZnO supported on activated carbon (AC) for dye degradation [63] has been explored. Table 2 summarizes the application of immobilized NMs for the removal of recalcitrant pollutants.

Table 2. Application of immobilized nanomaterials for the removal of recalcitrant pollutants.

| Immobilized NMs | Removed/Transformed Contaminants | Achievement | Reference |
|---------------------------------------|----------------------------------|--|-----------|
| Bioprocesses | | | |
| Pd in MEC | TCE | 93% removal efficiency vs. only 48% in the absence of Pd | [41] |
| Pd in AGS | IOP | 81% removal of IOP vs. only 61% in the absence of Pd | [37] |
| Pd in AGS | NP and Cr ⁶⁺ | Up to 20-fold higher conversion in Pd-amended system as compared to control without Pd | [39] |
| Pd in AGS | Azo dyes | Up to 10-fold increase in reduction rate as compared to control | [40] |
| GSC | NB | 30–50% higher removal of NB in the presence of graphene as compared to control | [42] |
| MGONS | IOP | 82% removal efficiency vs. only 51% in the absence of MGONS | [43] |
| Electrochemical systems | | | |
| Fe/Co in NPC | Organic pollutants | Removal of 91% within 60 min and mineralization efficiency of 90% within 240 min under neutral conditions, good stability and reusability, with low metal leaching | [55] |
| Fe ₃ O ₄ in MOF | Organic pollutants in OLL | 66.67% COD removal efficiency and degradation of heterocycles, phenols, and esters with increase in low-molecular-weight organics abundance | [56] |
| Cu-GOR in CF | DCF | 100% DCF degradation within 1 h at 1 V constant biased potential | [57] |
| Fe ₃ O ₄ in CCB | Dyes | Up to 2-fold increased degradation rate as compared to Fe ₃ O ₄ only | [49] |
| Photocatalytic applications | | | |
| La/TiO ₂ in L | DMP | 74.4% removal vs. only 60.1% in the absence of La and only 18.3% in the absence of La/TiO ₂ | [66] |
| Mn-CCMN | Dyes | Development of an effective and reusable photocatalyst for industrial wastewater treatment | [58] |
| ZnO in AC | Dyes | Promoting removal effect when adsorption and solar photocatalysis are simultaneously used for dye removal | [63] |

AC, activated carbon; AGS, anaerobic granular sludge; CCB, conductive carbon black; CCMN, chitosan conjugated magnetic nano-biocomposite; CF, carbon film; DCF, diclofenac; DMP, dimethyl phthalate; GSC, graphene-sludge composite; IOP, iopromide; L, lithium silicon powder; MEC, microbial electrolysis cell; MGONS, magnetic graphene oxide nano-sacs; MOF, metal organic framework; NB, nitrobenzene; NP, nitrophenol; NPC, nitrogen-doped porous carbon rods; OLL, old landfill leachate; GOR, reduced graphene oxide; TCE, tri-chloro-ethylene.

4. Immobilized NMs for the Removal of GHGs

Technologies to remove GHGs from industrial processes, such as fossil fuel extraction, as well as from wastewater treatment and landfill facilities, are currently mandatory to decrease these anthropogenic emanations, which are contributing to the overall warming of our planet. In the following sections, the role of immobilized NMs on the removal of

the three main GHGs (methane, nitrous oxide, and carbon dioxide) derived from human activities will be discussed.

4.1. Methane

While biogenic methane, produced from waste treatment, is considered a renewable energy source [14], there are important discharges of this gas during the exploitation of fossil energies. Additionally, methane is also released from wastewater-treatment plants and landfills. Methane is a powerful GHG with a global warming potential (GWP) 30-fold higher than that of carbon dioxide (CO₂); therefore, technologies to remove this gas from industrial emissions are demanded [67].

The catalytic oxidation of methane has been explored during the last decade and Pd-based catalysts have shown the highest activity for methane oxidation. Nevertheless, the application of these materials is still challenging due to poisoning by water and insufficient low-temperature performance. Recently, immobilized PdO_x on two-dimensional rafts showed efficient methane oxidation and water tolerance, creating a new venue of opportunities [68].

Metallic NPs have also been immobilized in electrochemical systems, which have been applied for the oxidation of methane to organic solvents, such as methanol, ethanol, and formate [69]. This strategy constitutes a green technology, turning a GHG into organic supplies required in several industrial sectors. NMs applied in electrochemical processes for this purpose include alloys composed of V, Pd, Au, Cu, Ru, and Ni, among others. Selectivity is still a challenge in these processes as the conversion efficiency largely varies from 30% up to 100% depending on the operational conditions and immobilized catalysts applied (Table 2). Lately, Pd-Pt NPs immobilized on ceria showed remarkable efficiency in completely oxidizing methane under wet conditions, which are relevant for automotive combustion; thus, these scientific findings could be the basis to install a technology to prevent methane emissions from vehicles [70].

Anaerobic methane oxidation by microorganisms using the anode of bio-electrochemical systems as a terminal electron acceptor has recently been reported [71–73]; thus, the doping of electrodes with catalytic metals could also enhance the anodic AOM activities previously observed, which also constitutes an interesting topic to study in future research for potential applications.

4.2. Nitrous Oxide (N₂O)

N₂O is a serious environmental threat causing the acidification of water reservoirs, ozone-layer depletion, and with a global warming potential (GWP) 300-fold higher than that of carbon dioxide (CO₂). Its concentration in the atmosphere has been augmented 18% since the preindustrial level, mainly due to human activities, such as the extensive application of fertilizers and burning of fossil fuels. Consequently, European Union edicts aim at its 42% reduction by 2030, with respect to 2013 emission data [74].

Selective catalytic reduction is the most successful and widely applied technology to mitigate N₂O emissions, where this GHG is removed by different reducing agents (e.g., hydrogen, ammonia, hydrocarbons) in the presence of metallic catalysts. Electrochemical processes have recently emerged as an encouraging option to reduce N₂O. Furthermore, the role of catalytic metals on the reduction in N₂O has also been explored with distinct alloys, containing Ir, Pd, Re, and La, among other elements, which showed promising efficiency [75–78].

More recently, the reduction of N₂O on the surface of electrodes, doped with NMs, was shown to be an effective strategy to remove this GHG from gas emissions in electrochemical systems. For instance, the deposition of Os and Pt NPs to create a stable film on the surface of different electrode materials was accomplished, and the doped electrodes were effective for reducing N₂O to dinitrogen gas (N₂) [79]. Lately, the reduction of N₂O to N₂ was also achieved on the surface of a cathode enriched with La, Sr, Fe, and Co [74]. The mechanism involved in this electrochemical process was elucidated, showing that the catalytic rate

returns to its open circuit value after polarization. The cathode was shown to remain stable during the operation; thus, it is proposed as a promising technology to remove N_2O from industrial exhaust emissions.

Considering that carbon-based materials, such as humic substances [80] and biochar (BC) [81], have been shown to effectively promote the reduction of N_2O by microbial communities, it is conceivable that carbonaceous NMs, such as GO, could also serve as effective materials, immobilized in biocathodes for the reduction of this GHG. Additionally, bio-Pd NPs have been applied in denitrifying processes for enhancing the reduction of nitrate to N_2 without N_2O accumulation, which could also serve as the basis for engineering biosystems preventing N_2O emissions from denitrifying processes [82]. Moreover, nZVI in the cathode of a bio-electrochemical system also enhances the reduction of nitrate without release of N_2O [83].

4.3. Carbon Dioxide (CO_2)

CO_2 is the principal GHG responsible for global warming and it is mainly produced from power plants. While carbon-capture facilities contribute to decrease the release of CO_2 from energy-generating infrastructure, the concentrated amines applied for this purpose are extremely toxic and difficult to treat after disposal [84]. Thus, green technologies are demanded to remove CO_2 from gas emissions, including those derived from WWTP, for instance for upgrading biogas.

NMs immobilized by different fixing strategies have recently been used for removing CO_2 from industrial gas streams. For example, nanocellulose-based membranes (NCM) have extensively been employed to eliminate this GHG. NCM offer great advantages for the removal of CO_2 , such as a high specific surface area, hydrophilicity, the option to modify their surface, environmental friendliness, and outstanding mechanical properties [85]. Since the diffusion mechanism involved in the separation of CO_2 through NCM occurs very slowly, there are several challenges still to be addressed for promoting their extensive application in industrial processes. Moreover, since pH is a crucial parameter during the removal of CO_2 in these processes, more studies are required for optimization. Additionally, NCM can also be doped with other NMs in order to enhance their performance, which will imply the optimization of membrane materials and tailoring of hybrid matrixes.

An exciting area of interest at present is the development of photo-bio-electrochemical systems, which involve the coupling between intact photosynthetic bacteria and electrodes, creating the proper niche to achieve “semi-artificial photosynthesis”, which may represent a new pathway for CO_2 sequestration. The interfacing of photosynthetic bacteria with modified electrode surfaces and metallic NPs promotes enhanced current densities [86]. For instance, Gacitua et al. [87] developed an Os-based redox polymer, which was combined with the cyanobacterium, *Gloeocapsopsis* sp. UTEXB3054, achieving a photo-current density of $2.3 \mu A/cm^2$. Furthermore, Liu and Choi (2021) [88] reported the combination of biogenic Au NPs with *Synechocystis* sp. in a process which yielded $120 \mu A/cm^2$. An additional benefit of applying photo-bio-electrochemical systems for CO_2 sequestration is the production of photosynthetic biomass with the proper oil content to produce biofuels. Therefore, there is a whole avenue opened for applying NMs in photo-bio-electrochemical systems, which may provide multiple environmental services.

5. Immobilized NMs for Adsorption Processes

Adsorption processes are one of the technologies applied the most for the attenuation of environmental pollution. It is a traditional methodology based on the physicochemical interactions between the adsorbent/adsorbate that can be maximized using specific materials with a variety of tailored textural, mechanical, chemical, and electrical properties. Additionally, operational, economical, and environmental issues must be concerned during the selection and implementation of the adsorption system. Currently, the emergence of functional NMs and their innovative properties have gained attention as potential alternatives for environmental applications. The production of a broad range of nanocomposites

has opened an unprecedented technological opportunity for a variety of applications, including adsorption, over the conventional use of these materials [89]. The use of immobilized NMs in adsorption processes includes the conjugation of NPs and support characteristics for a correct adsorptive performance. Many materials from different sources (carbon, silica, polymers) have been explored as NP carriers, including more innovative and sophisticated structures, such as graphene, biopolymers, CNT, MOF, aerogels and hydrogels, magnetic materials, quantum dots, and some hybrids integrating some of the previously mentioned materials [90–95]. Recently developed nanocomposites used for adsorption purposes are reviewed in this section with an emphasis on the type of immobilized NMs, host material, specific surface area (SSA), and adsorption capacity (Q) of different pollutants. Figure 3 schematizes the use of immobilized NMs for the treatment of polluted streams through adsorption processes.

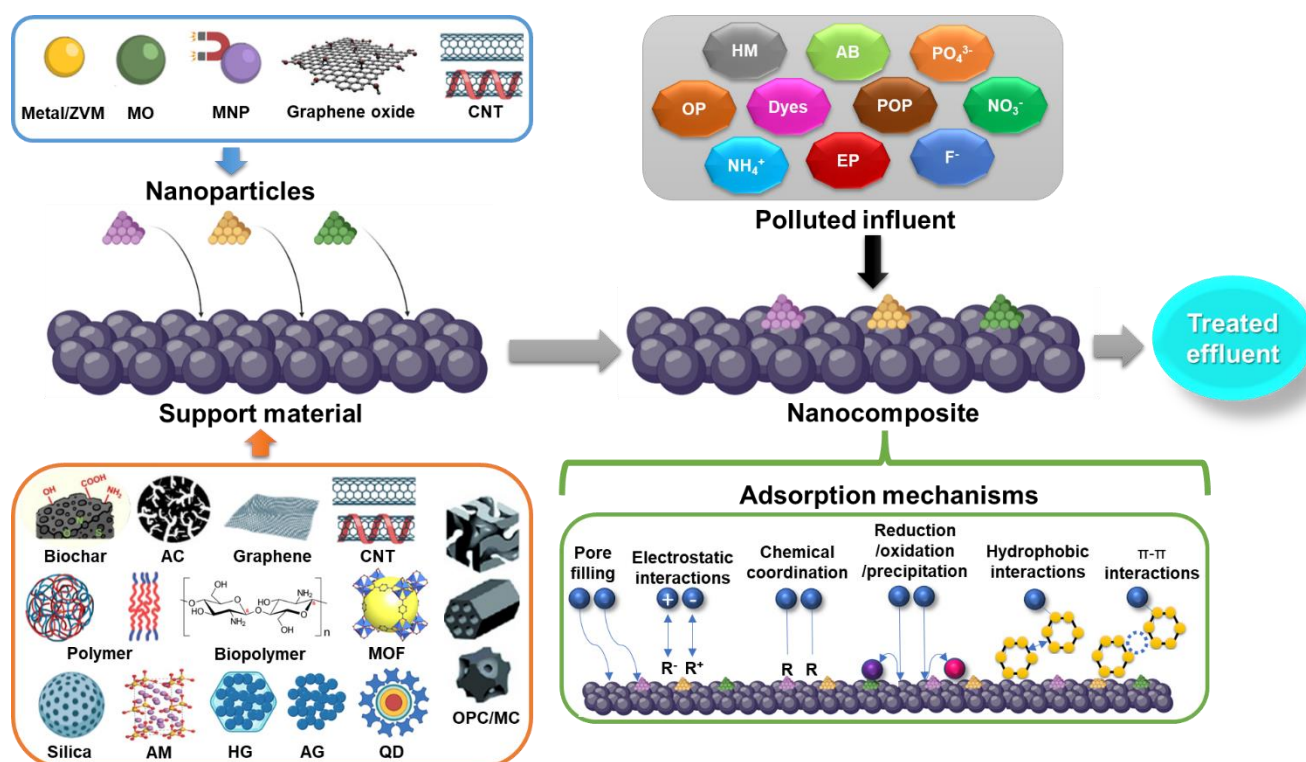


Figure 3. Scheme of nanoparticle immobilization on different supporting materials for the treatment of polluted discharges through adsorption processes. AB, antibiotic; AC, activated carbon; AG, aerogel; AM, alkali-metal-based material; CNT, carbon nanotube; EP, emerging pollutant; HG, hydrogel; HM, heavy metal; MC, monolithic carbon; MO, metal oxide; MOF, metal organic framework; MNP, magnetic nanoparticle; OP, organic pollutant; OPC, ordered porous carbon; POP, persistent organic pollutant; QD, quantum dot; ZVM, zero valent metal.

5.1. Carbon-Based Nanocomposites

Their outstanding physical and chemical properties, coupled to their recognized versatility and stability under a variety of working conditions, make carbon-based materials an ideal option as a host material for NM immobilization. The large specific surface area, high pore volume, hydrophobic nature, high electrical conductivity, chemical inertness, and vast chemical functionality enables the loading of NPs through the carbonaceous matrix for successful applications in environmental remediation, energy storage, and catalysis [89,96,97]. AC is one of the most frequently used adsorbents for the removal of numerous pollutants from water and air bodies, mainly due to its high specific surface area, reaching values of 2878 m²/g for chemical activation with KOH and 2213 m²/g for steam activation [98], a characteristic that renders them suitable for the immobilization

of a variety of NPs [99,100]. In the same way, BC has emerged as a low-cost alternative for metal NP immobilization [101], including the environmental and economic benefits associated with the use of biomass waste materials instead of non-renewable sources for AC production [102]. The intensive use of BC as a host material for NP immobilization is reflected in a recent review that summarized its performance as an nZVI support for heavy metal adsorption [103], and another focused on the preparation, environmental application, and prospect of BC-supported metal NPs [101]. Many sources for BC production, such as wood, coconut shell, corn straw, rice husk, nutshell, and peach stone, among others, have been explored, mainly based on their carbon content, abundance, inherent environmental issues, and mechanical properties [99,101,104]. Immobilization of NPs into a BC structure can enhance the advantages and overcome the drawbacks of both materials in terms of the distribution and stabilization of loaded metals, reducing the aggregation of NPs, their leaching and surface passivation, increasing the disposable active sites and oxygenated functional groups, and improving the catalytic/redox performance and their thermal stability [101,105,106].

Many pollutants have been targeted for remediation by adsorption using carbon-based nanocomposites. The removal of metal ions and dyes is one of the major areas of research for the use of porous materials, such as AC and BC, as well as carbon-based nanocomposites [107]. However, studies related to the removal of organic compounds (pesticides, antibiotics, and persistent organic pollutants), and inorganic species (phosphate, fluoride, ammonium, nitrate, etc.), have been recently reported for the treatment and remediation of water bodies and contaminated soils [83,100,108–111]. The properties of carbon materials used as supports are strongly affected by the integration of a variety of NPs, depending on the immobilization procedure (pre- or post-synthesis), modification treatment, and thermal processes applied. Physicochemical changes in terms of specific surface area, pore volume, pore size, functionality, ion-exchange capacity, conductivity, and reactivity are denoted on the resulting nanocomposite. Generally, the surface area for carbonaceous materials shows a general decline with the degree of modification and/or functionalization, while the adsorption capacity is increased [112]. NMs, including metal NPs such as Fe, Cu, Au, Pt, Pd, Ru, Ag, Co, and Ni, are the subject of great scientific and economic interest for oil-refining, chemical-manufacturing, and environmental catalysis applications [96]. In adsorption processes for the removal of heavy metals from contaminated water, iron and iron oxide NPs, immobilized in carbonaceous matrixes, have been extensively described, such as Cd^{2+} , Cu^{2+} , Ni^{2+} , Co^{2+} , Cr^{6+} , Pb^{2+} , As^{3+} , and Hg^{2+} [103,113]. Additionally, the inclusion of metal NPs, such as MgO, CaO, Fe_2O_3 , Al_2O_3 , Fe^0 , and Ag^0 , on carbon nanocomposites can successfully improve the ligand-binding density by increasing the positive charge, allowing the higher removal of inorganic compounds than raw carbon materials [101]. Adsorption processes with carbon-based nanocomposites are also applicable for contaminated soils and air-pollution treatment. In the case of GHGs, nanocomposites using cocoa shell with amino groups and immobilized cobalt NPs were reported to effectively increase the CO_2 adsorption capacity from 0.015 to 0.24 mmol/g [114], or in the case of soil remediation, modified magnetic BC was promisingly applied in the immobilization of heavy metals for the remediation of a multi-contaminated soil [115].

5.2. Silica-Based Nanocomposites

Silica (SiO_2) is one of the commonly used supports for NP immobilization. Santa Barbara amorphous-type material (SBA-15) and Mobil Composition of Matter (MCM-41) are the most common types of amorphous-ordered, mesoporous silicas used as support in catalytic applications due to their extraordinary textural properties. Tetraethyl orthosilicate (TEOS) is the most common precursor for these ordered mesoporous silicas by reacting it with a template made of micellar rods or using sol-gel methodology [96]. Moreover, synthesis through the Stöber method and reverse micro-emulsion method yields materials with a controllable size, shape, and structure. Silica-based materials have gained attention as a scaffold or matrix for different NMs due to their superior properties, such as chemical

inertness, thermal stability, transparent to light and magnetism, lower van der Waals interactions, water-solubility, nontoxicity, and biocompatibility, over their counterparts [116]. Additionally, these materials have a high adsorption capacity, low permeability, high chemical and mechanical stability, large surface area, and narrow pore-size distributions [117]. The aforementioned characteristics render silica composites suitable for optical, magnetic, electrical, biomedical, environmental, and catalytic applications [118]. Table 3 summarizes several reports about the use of NMs for the adsorption of different pollutants.

Table 3. Adsorption of pollutants using immobilized nanomaterials.

| Supporting Material | Nanomaterial | Pollutants | Q (mg/g) | | SSA (m ² /g) | | Reference |
|---------------------|--|--|--------------|------------------------|-------------------------|-----------|-----------|
| | | | Support | Composite | Support | Composite | |
| A-Chitosan | Ni ²⁺ | Pb ²⁺ | 21.0 | 50.3 | NA | NA | [119] |
| Bamboo BC | MgO | Phosphate | 1.3 | 370 | NA | 399 | [120] |
| Chitosan | Fe ⁰ | Bisphenol-A | NA | 65.2 | NA | NA | [121] |
| Chitosan | Bio-CuO | Congo red, Eriochrome black T | NA | 119.7, 235.7 | 15.84 | 25.3 | [122] |
| CNT | MgO | Hg ²⁺ | NA | 58.8 | 91.3 | 110.4 | [90] |
| Corn stem BC | Fe-Mn | As ²⁺ | 2.9 | 8.3 | 60.9 | 208.6 | [123] |
| Douglas fir BC | α-Fe ₂ O ₃ , Fe ₃ O ₄ | Nitrate, fluoride | NA | 15.5, 9.0 | 663 | 494 | [124] |
| HCS BC | Fe ⁰ | Pb ²⁺ , Cu ²⁺ , Zn ²⁺ | NA | 195.1, 161.9, 109.7 | 1216 | 603.4 | [125] |
| MOF-WC | Co | Congo red, Methylene blue | 613.6, 469.5 | 1117.0, 805.1 | NA | 170.4 | [126] |
| Polydopamine | Graphene and Fe ₃ O ₄ | Methylene blue | 110 | 140.3 | NA | 85.6 | [127] |
| PC | Co | Sr ²⁺ | NA | 3.21 | NA | NA | [128] |
| Silica | HC | Cd ²⁺ , Pb ²⁺ , Ni ²⁺ | NA | 0.5, 8.9, 13.5 | 195 | 197 | [129] |
| Silica | Au | Toluene | NA | 1360 | 465.3 | 367.4 | [130] |
| Silica aerogel | La(OH) ₃ | Phosphate | 19.2 | 153.8 | 561.0 | 252.7 | [95] |

A, aminophosphorylated; BC, biochar; CNT, carbon nanotubes carbon; HC, hydrophilic carbon; HCS, hydrophilic corn stalk; MOF-WC, metal-organic-framework wood composite; NA, not available; PC, phosphorylated chitosan.

The insertion of NMs onto siliceous matrixes changes and increases the desired properties of the resultant nanocomposites, since their main functions are mostly determined by such NMs, but provides an inert, transparent, stable, and heterogenous support. The sufficiently large pore size of mesoporous silica and the high density of silanol groups allows the integration of large molecules, surface functionalization, and the introduction of a variety of NPs for their application in catalysis, ion exchange, sensing, and adsorption, where stereochemical configurations, charge densities, specific binding sites, and acidities are needed. In adsorption processes, the attachment of NPs or a specific functionality onto an inert high specific surface area creates active sites for the selective adsorption of the target species. Several metal NPs (Pd, Ag, Ni, etc.) have been successfully immobilized on silica materials, such as aerogels, spheres, emulsions, zeolites, aluminosilicates, and clays [131–135]. The use of silica-based NMs has been extended to the adsorption and separation of hazardous metal ions, radioactive nuclides, or minor actinides from wastewater and high-level radioactive waste [136]. Recent studies have reported the use of nano-copper supported on mesoporous silica for the adsorption of dibenzothiophene in fuel oils [137]. Furthermore, the immobilization of hydrophilic NPs, derived from carbon black, on silica beads to enhance the removal of Cd²⁺, Ni²⁺, and Pb²⁺ [129] has been revealed. Additionally, silica aerogel composites embedded with nano lanthanum hydroxide to promote the removal of phosphate [95] have recently been reported. Furthermore, the use of gold NPs supported on amido-amidoxime-functionalized silica for toluene-vapor adsorption [130] and the sequestration of heavy metal ions from aqueous solutions using biosynthesized silica-based zinc oxide nanocomposites with agricultural wastes as a source of silica [138] have been explored.

5.3. Polymer-Based Nanocomposites

Polymer nanocomposites consist of a polymer or a copolymer, filled with synthetic or natural inorganic compounds to improve their chemical and physical properties or to reduce costs by acting as a diluent for the polymer [139]. The resultant nanocomposites combine the inherent nanoparticle qualities with the stability, controlled pore size, and surface chemistry of the polymeric matrix, including the benefits provided for the mechanical, thermal, optical, and electronic properties of such host material [140]. Several polymers have been used as supporting materials, including chitosan, porous resins, alginate, gelatin, and cellulose, for the immobilization of a variety of NPs, such as metallic oxides, zero-valent metals, single-enzyme NPs, among others [141–143]. Additionally, some NMs, such as reduced GO nanosheets, have been used for the self-assembling of nanostructured polymer composites [144]. The variety and availability of polymer-based nanocomposites and the high interfacial activity of the nanofillers makes them suitable for environmental remediation, catalytic degradation, detection and sensing, and green chemistry, among other applications [145–147]. The enhanced removal efficiencies of numerous toxic and recalcitrant pollutants, such as dyes (indigo carmine, methyl orange, methylene blue, crystal violet, reactive black, malachite green), heavy metal ions (Cr^{2+} , Pb^{2+} , As, Co, Ni^{2+} , Cu, V, Sr^{2+} , Hg^{2+}), and organic molecules (diclofenac, nitrobenzene, trichlorophenol) have been reported using adsorbent-based polymeric nanocomposites [127,128,140,146,148]. Moreover, the selective adsorption of some species in the presence of competitors has been successfully tested [149]. MOFs are a subclass of coordination polymers with inorganic nodes bonded by organic ligands building a 3D spongy structure [111]. As a new functional material that combines an ultra-high SSA (up to $5900 \text{ m}^2/\text{g}$) with high modularity, varied functionality, and strong metal–ligand interactions [96,111], MOFs have a wide application prospect in adsorption, separation, and gas storage [126], as well as their suitability for supporting active NPs for environmental remediation and catalytic purposes [150,151].

6. Conclusions

This article provides an overview of the vibrant and increasing scientific interest that has been awoken in manufacturing engineered NMs, which have been immobilized in different matrixes, for environmental applications. These purposes include their use for producing renewable energies through biological and electrochemical systems, as well as the removal of priority contaminants and GHGs from industrial discharges by microbial and physicochemical processes. There certainly are several avenues of opportunities to expand the application of immobilized NMs for environmental processes, which deserve consideration in future works. For instance, efforts should be made towards optimizing the immobilization of NMs in different matrixes to prevent their detachment during environmental applications. The tailoring of nanocomposites, integrating the catalytic properties of distinct NMs, should also be explored for electrochemical and catalytic processes intended for removing recalcitrant contaminants and GHGs. Finally, strategies to regenerate NMs to promote their recycling during their applications are also demanded.

Author Contributions: Conceptualization, F.J.C.; validation, F.J.C. and L.A.R.-M.; formal analysis, F.J.C. and L.A.R.-M.; data curation, F.J.C. and L.A.R.-M.; writing—original draft preparation, F.J.C. and L.A.R.-M.; writing—review and editing, F.J.C.; visualization, F.J.C.; supervision, F.J.C.; project administration, F.J.C.; funding acquisition, F.J.C. All authors have read and agreed to the published version of the manuscript.

Funding: This research was funded by Universidad Nacional Autónoma de México (UNAM, PAPIIT grant TA200122) and by a fellow from UNAM (DGAPA grant number COIC/DDTPA/064/2020) to LARM.

Informed Consent Statement: Not applicable.

Data Availability Statement: Not applicable.

Acknowledgments: F.J.C. acknowledges financial support from Universidad Nacional Autónoma de México (UNAM, PAPIIT grant TA200122). LARM acknowledges a fellow from UNAM (DGAPA grant number COIC/DDTPA/064/2020).

Conflicts of Interest: The authors declare no conflict of interest.

References

1. Pat-Espadas, A.M.; Cervantes, F.J. Microbial Recovery of Metallic Nanoparticles from Industrial Wastes and Their Environmental Applications. *J. Chem. Technol. Biotechnol.* **2018**, *93*, 3091–3112. [[CrossRef](#)]
2. Aghababai, A.; Jabbari, H. Results in Engineering Nanomaterials for Environmental Applications. *Results Eng.* **2022**, *15*, 100467. [[CrossRef](#)]
3. Ganguly, P.; Breen, A.; Pillai, S.C. Toxicity of Nanomaterials: Exposure, Pathways, Assessment, and Recent Advances. *ACS Biomater. Sci. Eng.* **2018**, *4*, 2237–2275. [[CrossRef](#)] [[PubMed](#)]
4. Srikanth, B.; Goutham, R.; Badri Narayan, R.; Ramprasath, A.; Gopinath, K.P.; Sankaranarayanan, A.R. Recent Advancements in Supporting Materials for Immobilised Photocatalytic Applications in Waste Water Treatment. *J. Environ. Manag.* **2017**, *200*, 60–78. [[CrossRef](#)]
5. Park, J.-H.; Kang, H.-J.; Park, K.-H.; Park, H.-D. Direct Interspecies Electron Transfer via Conductive Materials: A Perspective for Anaerobic Digestion Applications. *Bioresour. Technol.* **2018**, *254*, 300–311. [[CrossRef](#)] [[PubMed](#)]
6. Martins, G.; Salvador, A.F.; Pereira, L.; Alves, M.M. Methane Production and Conductive Materials: A Critical Review. *Environ. Sci. Technol.* **2018**, *52*, 10241–10253. [[CrossRef](#)] [[PubMed](#)]
7. Rotaru, A.E.; Shrestha, P.M.; Liu, F.; Markovaite, B.; Chen, S.; Nevin, K.P.; Lovley, D.R. Direct Interspecies Electron Transfer between *Geobacter Metallireducens* and *Methanosarcina Barkeri*. *Appl. Environ. Microbiol.* **2014**, *80*, 4599–4605. [[CrossRef](#)] [[PubMed](#)]
8. Chen, S.; Rotaru, A.E.; Shrestha, P.M.; Malvankar, N.S.; Liu, F.; Fan, W.; Nevin, K.P.; Lovley, D.R. Promoting Interspecies Electron Transfer with Biochar. *Sci. Rep.* **2014**, *4*, 1–7. [[CrossRef](#)]
9. De Velasco-Maldonado, P.S.; Pat-Espadas, A.M.; Cházaro-Ruiz, L.F.; Cervantes, F.J.; Hernández-Montoya, V. Cold Oxygen Plasma Induces Changes on the Surface of Carbon Materials Enhancing Methanogenesis and N₂O Reduction in Anaerobic Sludge Incubations. *J. Chem. Technol. Biotechnol.* **2019**, *94*, 3367–3374. [[CrossRef](#)]
10. Bueno-López, J.I.; Rangel-Mendez, J.R.; Alatraste-Mondragón, F.; Pérez-Rodríguez, F.; Hernández-Montoya, V.; Cervantes, F.J. Graphene Oxide Triggers Mass Transfer Limitations on the Methanogenic Activity of an Anaerobic Consortium with a Particulate Substrate. *Chemosphere* **2018**, *211*, 709–716. [[CrossRef](#)] [[PubMed](#)]
11. Bueno-López, J.I.; Díaz-Hinojosa, A.; Rangel-Mendez, J.R.; Alatraste-Mondragón, F.; Pérez-Rodríguez, F.; Hernández-Montoya, V.; Cervantes, F.J. Methane Production Enhanced by Reduced Graphene Oxide in an Anaerobic Consortium Supplied with Particulate and Soluble Substrates. *J. Chem. Technol. Biotechnol.* **2020**, *95*, 2983–2990. [[CrossRef](#)]
12. Song, X.; Liu, J.; Jiang, Q.; Zhang, P.; Shao, Y.; He, W.; Feng, Y. Enhanced Electron Transfer and Methane Production from Low-Strength Wastewater Using a New Granular Activated Carbon Modified with Nano-Fe₃O₄. *Chem. Eng. J.* **2019**, *374*, 1344–1352. [[CrossRef](#)]
13. Zheng, Y.; Quan, X.; Zhuo, M.; Zhang, X.; Quan, Y. In-Situ Formation and Self-Immobilization of Biogenic Fe Oxides in Anaerobic Granular Sludge for Enhanced Performance of Acidogenesis and Methanogenesis. *Sci. Total Environ.* **2021**, *787*, 147400. [[CrossRef](#)] [[PubMed](#)]
14. Ramírez-Montoya, L.A.; Montes-Morán, M.A.; Rangel-Mendez, J.R.; Cervantes, F.J. Enhanced Anaerobic Treatment of Synthetic Protein-Rich Wastewater Promoted by Organic Xerogels. *Biodegradation* **2022**, *33*, 255–265. [[CrossRef](#)] [[PubMed](#)]
15. Serrato-Nerio, H.E.; Díaz-Hinojosa, A.; Cervantes, F.J. Vacuum-Assisted Production of Hydrogen and Volatile Fatty Acids from Lignocellulosic Biomass Derived from Energy-Crops Pruning. *Int. J. Hydrogen Energy* **2020**, *45*, 28499–28504. [[CrossRef](#)]
16. Zhang, Y.; Shen, J. Enhancement Effect of Gold Nanoparticles on Biohydrogen Production from Artificial Wastewater. *Int. J. Hydrogen Energy* **2007**, *32*, 17–23. [[CrossRef](#)]
17. Zhao, W.; Zhang, Y.; Du, B.; Wei, D.; Wei, Q.; Zhao, Y. Enhancement Effect of Silver Nanoparticles on Fermentative Biohydrogen Production Using Mixed Bacteria. *Bioresour. Technol.* **2013**, *142*, 240–245. [[CrossRef](#)] [[PubMed](#)]
18. Engliman, N.S.; Abdul, P.M.; Wu, S.-Y.; Jahim, J.M. Influence of Iron (II) Oxide Nanoparticle on Biohydrogen Production in Thermophilic Mixed Fermentation. *Int. J. Hydrogen Energy* **2017**, *42*, 27482–27493. [[CrossRef](#)]
19. Elreedy, A.; Ibrahim, E.; Hassan, N.; El-Dissouky, A.; Fujii, M.; Yoshimura, C.; Tawfik, A. Nickel-Graphene Nanocomposite as a Novel Supplement for Enhancement of Biohydrogen Production from Industrial Wastewater Containing Mono-Ethylene Glycol. *Energy Convers. Manag.* **2017**, *140*, 133–144. [[CrossRef](#)]
20. Boshagh, F.; Rostami, K.; Moazami, N. Biohydrogen Production by Immobilized Enterobacter Aerogenes on Functionalized Multi-Walled Carbon Nanotube. *Int. J. Hydrogen Energy* **2019**, *44*, 14395–14405. [[CrossRef](#)]
21. Arya, I.; Poona, A.; Dikshit, P.K.; Pandit, S.; Kumar, J.; Singh, H.N.; Jha, N.K.; Rudayni, H.A.; Chaudhary, A.A.; Kumar, S. Current Trends and Future Prospects of Nanotechnology in Biofuel Production. *Catalysts* **2021**, *11*, 1308. [[CrossRef](#)]
22. Lee, K.H.; Choi, I.S.; Kim, Y.-G.; Yang, D.-J.; Bae, H.-J. Enhanced Production of Bioethanol and Ultrastructural Characteristics of Reused *Saccharomyces Cerevisiae* Immobilized Calcium Alginate Beads. *Bioresour. Technol.* **2011**, *102*, 8191–8198. [[CrossRef](#)] [[PubMed](#)]

23. Brinchi, L.; Cotana, F.; Fortunati, E.; Kenny, J.M. Production of Nanocrystalline Cellulose from Lignocellulosic Biomass: Technology and Applications. *Carbohydr. Polym.* **2013**, *94*, 154–169. [[CrossRef](#)] [[PubMed](#)]
24. Chen, Y.; Liu, T.; He, H.; Liang, H. Fe₃O₄/ZnMg(Al)O Magnetic Nanoparticles for Efficient Biodiesel Production. *Appl. Organomet. Chem.* **2018**, *32*, e4330. [[CrossRef](#)]
25. Orozco, R.L.; Redwood, M.D.; Yong, P.; Caldeleri, I.; Sargent, F.; Macaskie, L.E. Towards an Integrated System for Bio-Energy: Hydrogen Production by Escherichia Coli and Use of Palladium-Coated Waste Cells for Electricity Generation in a Fuel Cell. *Biotechnol. Lett.* **2010**, *32*, 1837–1845. [[CrossRef](#)]
26. Bunge, M.; Søjbjerg, L.S.; Rotaru, A.-E.; Gauthier, D.; Lindhardt, A.T.; Hause, G.; Finster, K.; Kingshott, P.; Skrydstrup, T.; Meyer, R.L. Formation of Palladium(0) Nanoparticles at Microbial Surfaces. *Biotechnol. Bioeng.* **2010**, *107*, 206–215. [[CrossRef](#)]
27. Yong, P.; Mikheenko, I.P.; Deplanche, K.; Redwood, M.D.; Macaskie, L.E. Biorefining of Precious Metals from Wastes: An Answer to Manufacturing of Cheap Nanocatalysts for Fuel Cells and Power Generation via an Integrated Biorefinery? *Biotechnol. Lett.* **2010**, *32*, 1821–1828. [[CrossRef](#)]
28. Ogi, T.; Honda, R.; Tamaoki, K.; Saitoh, N.; Konishi, Y. Direct Room-Temperature Synthesis of a Highly Dispersed Pd Nanoparticle Catalyst and Its Electrical Properties in a Fuel Cell. *Powder Technol.* **2011**, *205*, 143–148. [[CrossRef](#)]
29. Dimitriadis, S.; Nomikou, N.; McHale, A.P. Pt-Based Electro-Catalytic Materials Derived from Biosorption Processes and Their Exploitation in Fuel Cell Technology. *Biotechnol. Lett.* **2007**, *29*, 545–551. [[CrossRef](#)]
30. Li, Q.; Mahmood, N.; Zhu, J.; Hou, Y.; Sun, S. Graphene and Its Composites with Nanoparticles for Electrochemical Energy Applications. *Nano Today* **2014**, *9*, 668–683. [[CrossRef](#)]
31. Wang, Y.; Wu, J.; Tang, Y.; Lü, X.; Yang, C.; Qin, M.; Huang, F.; Li, X.; Zhang, X. Phase-Controlled Synthesis of Cobalt Sulfides for Lithium Ion Batteries. *ACS Appl. Mater. Interfaces* **2012**, *4*, 4246–4250. [[CrossRef](#)]
32. Mahmood, N.; Zhang, C.; Jiang, J.; Liu, F.; Hou, Y. Multifunctional Co₃S₄/Graphene Composites for Lithium Ion Batteries and Oxygen Reduction Reaction. *Chem. Eur. J.* **2013**, *19*, 5183–5190. [[CrossRef](#)]
33. Yang, X.; Zhu, J.; Qiu, L.; Li, D. Bioinspired Effective Prevention of Restacking in Multilayered Graphene Films: Towards the Next Generation of High-Performance Supercapacitors. *Adv. Mat.* **2011**, *23*, 2833–2838. [[CrossRef](#)]
34. Ji, J.; Zhang, L.L.; Ji, H.; Li, Y.; Zhao, X.; Bai, X.; Fan, X.; Zhang, F.; Ruoff, R.S. Nanoporous Ni(OH)₂ Thin Film on 3D Ultrathin-Graphite Foam for Asymmetric Supercapacitor. *ACS Nano* **2013**, *7*, 6237–6243. [[CrossRef](#)]
35. Canal-Rodríguez, M.; Arenillas, A.; Rey-Raap, N.; Ramos-Fernández, G.; Martín-Gullón, I.; Menéndez, J.A. Graphene-Doped Carbon Xerogel Combining High Electrical Conductivity and Surface Area for Optimized Aqueous Supercapacitors. *Carbon* **2017**, *118*, 291–298. [[CrossRef](#)]
36. Martínez-Lázaro, A.; Ramírez-Montoya, L.A.; Ledesma-García, J.; Montes-Morán, M.A.; Gurrola, M.P.; Menéndez, J.A.; Arenillas, A.; Arriaga, L.G. Facile Synthesis of Unsupported Pd Aerogel for High Performance Formic Acid Microfluidic Fuel Cell. *Materials* **2022**, *15*, 1422. [[CrossRef](#)]
37. Pat-Espadas, A.M.; Razo-Flores, E.; Rangel-Mendez, J.R.; Ascacio-Valdes, J.A.; Aguilar, C.N.; Cervantes, F.J. Immobilization of Biogenic Pd(0) in Anaerobic Granular Sludge for the Biotransformation of Recalcitrant Halogenated Pollutants in UASB Reactors. *Appl. Microbiol. Biotechnol.* **2016**, *100*, 1427–1436. [[CrossRef](#)] [[PubMed](#)]
38. De Corte, S.; Hennebel, T.; De Gussem, B.; Verstraete, W.; Boon, N. Bio-Palladium: From Metal Recovery to Catalytic Applications. *Microb. Biotechnol.* **2012**, *5*, 5–17. [[CrossRef](#)]
39. Suja, E.; Nancharaiyah, Y.V.; Venugopalan, V.P. Biogenic Nanopalladium Production by Self-Immobilized Granular Biomass: Application for Contaminant Remediation. *Water Res.* **2014**, *65*, 395–401. [[CrossRef](#)]
40. Quan, X.; Zhang, X.; Xu, H. In-Situ Formation and Immobilization of Biogenic Nanopalladium into Anaerobic Granular Sludge Enhances Azo Dyes Degradation. *Water Res.* **2015**, *78*, 74–83. [[CrossRef](#)] [[PubMed](#)]
41. Hennebel, T.; Benner, J.; Clauwaert, P.; Vanhaecke, L.; Aelterman, P.; Callebaut, R.; Boon, N.; Verstraete, W. Dehalogenation of Environmental Pollutants in Microbial Electrolysis Cells with Biogenic Palladium Nanoparticles. *Biotechnol. Lett.* **2011**, *33*, 89–95. [[CrossRef](#)] [[PubMed](#)]
42. Wang, J.; Wang, D.; Liu, G.; Jin, R.; Lu, H. Enhanced Nitrobenzene Biotransformation by Graphene-Anaerobic Sludge Composite. *J. Chem. Technol. Biotechnol.* **2014**, *89*, 750–755. [[CrossRef](#)]
43. Toral-Sánchez, E.; Rangel-Mendez, J.R.; Hurt, R.H.; Ascacio Valdés, J.A.; Aguilar, C.N.; Cervantes, F.J. Novel Application of Magnetic Nano-Carbon Composite as Redox Mediator in the Reductive Biodegradation of Iopromide in Anaerobic Continuous Systems. *Appl. Microbiol. Biotechnol.* **2018**, *102*, 8951–8961. [[CrossRef](#)]
44. Alvarez, L.H.; Perez-Cruz, M.A.; Rangel-Mendez, J.R.; Cervantes, F.J. Immobilized Redox Mediator on Metal-Oxides Nanoparticles and Its Catalytic Effect in a Reductive Decolorization Process. *J. Hazard. Mater.* **2010**, *184*, 268–272. [[CrossRef](#)]
45. Alvarez, L.H.; Jimenez-Bermudez, L.; Hernandez-Montoya, V.; Cervantes, F.J. Enhanced Dechlorination of Carbon Tetrachloride by Immobilized Fulvic Acids on Alumina Particles. *Water Air Soil Poll* **2012**, *223*, 1911–1920. [[CrossRef](#)]
46. Cervantes, F.J.; Gómez, R.; Alvarez, L.H.; Martinez, C.M.; Hernandez-Montoya, V. Efficient Anaerobic Treatment of Synthetic Textile Wastewater in a UASB Reactor with Granular Sludge Enriched with Humic Acids Supported on Alumina Nanoparticles. *Biodegradation* **2015**, *26*, 289–298. [[CrossRef](#)]
47. Guobin, S.; Huaiying, Z.; Weiquan, C.; Jianmin, X.; Huizhou, L. Improvement of Biodesulfurization Rate by Assembling Nanosorbents on the Surfaces of Microbial Cells. *Biophys. J.* **2005**, *89*, L58–L60. [[CrossRef](#)]

48. Särkkä, H.; Bhatnagar, A.; Sillanpää, M. Recent Developments of Electro-Oxidation in Water Treatment—A Review. *J. Electroanal. Chem.* **2015**, *754*, 46–56. [[CrossRef](#)]
49. Sun, M.; Zhao, Y.; Ge, H. Electrocatalytic Degradation of Methyl Orange Using Nano-Fe₃O₄ Supported on Conductive Carbon Black as Particle Electrode. *Int. J. Electrochem. Sci.* **2022**, *17*, 1–20. [[CrossRef](#)]
50. Ouarda, Y.; Trellu, C.; Lesage, G.; Rivallin, M.; Drogui, P.; Cretin, M. Electro-Oxidation of Secondary Effluents from Various Wastewater Plants for the Removal of Acetaminophen and Dissolved Organic Matter. *Sci. Total Environ.* **2020**, *738*, 140352. [[CrossRef](#)]
51. Annabi, C.; Fourcade, F.; Soutrel, I.; Geneste, F.; Floner, D.; Bellakhal, N.; Amrane, A. Degradation of Enoxacin Antibiotic by the Electro-Fenton Process: Optimization, Biodegradability Improvement and Degradation Mechanism. *J. Environ. Manag.* **2016**, *165*, 96–105. [[CrossRef](#)]
52. He, K.; Chen, G.; Zeng, G.; Chen, A.; Huang, Z.; Shi, J.; Huang, T.; Peng, M.; Hu, L. Three-Dimensional Graphene Supported Catalysts for Organic Dyes Degradation. *Appl. Catal. B* **2018**, *228*, 19–28. [[CrossRef](#)]
53. Rahmani, A.; Salari, M.; Tari, K.; Shabanloo, A.; Shabanloo, N.; Bajalan, S. Enhanced Degradation of Furfural by Heat-Activated Persulfate/nZVI-rGO Oxidation System: Degradation Pathway and Improving the Biodegradability of Oil Refinery Wastewater. *J. Environ. Chem. Eng.* **2020**, *8*, 104468. [[CrossRef](#)]
54. Wang, Z.; Song, B.; Li, J.; Teng, X. Chemosphere Degradation of Norfloxacin Wastewater Using Kaolin/Steel Slag Particle Electrodes: Performance, Mechanism and Pathway. *Chemosphere* **2021**, *270*, 128652. [[CrossRef](#)]
55. Hu, T.; Deng, F.; Feng, H.; Zhang, J.; Shao, B.; Feng, C.; Tang, W.; Tang, L. Fe/Co Bimetallic Nanoparticles Embedded in MOF-Derived Nitrogen-Doped Porous Carbon Rods as Efficient Heterogeneous Electro-Fenton Catalysts for Degradation of Organic Pollutants. *Appl. Mater. Today* **2021**, *24*, 101161. [[CrossRef](#)]
56. He, Z.; Liu, Y.; Wang, J.; Lv, Y.; Xu, Y.; Jia, S. Enhanced Degradation of Old Landfill Leachate in Heterogeneous Electro-Fenton Catalyzed Using Fe₃O₄ Nano-Particles Encapsulated by Metal Organic Frameworks. *J. Clean Prod.* **2021**, *321*, 128947. [[CrossRef](#)]
57. Kumar, A.; Omar, R.A.; Verma, N. Efficient Electro-Oxidation of Diclofenac Persistent Organic Pollutant in Wastewater Using Carbon Film-Supported Cu-rGO Electrode. *Chemosphere* **2020**, *248*, 126030. [[CrossRef](#)]
58. Yang, Y.; Khan, H.; Gao, S.; Khalil, A.K.; Ali, N.; Khan, A.; Show, P.L.; Bilal, M.; Khan, H. Fabrication, Characterization, and Photocatalytic Degradation Potential of Chitosan-Conjugated Manganese Magnetic Nano-Biocomposite for Emerging Dye Pollutants. *Chemosphere* **2022**, *306*, 135647. [[CrossRef](#)]
59. Garrido-Cardenas, J.A.; Esteban-García, B.; Agüera, A.; Sánchez-Pérez, J.A.; Manzano-Agugliaro, F. Wastewater Treatment by Advanced Oxidation Process and Their Worldwide Research Trends. *Int. J. Env. Res. Public Health* **2020**, *17*, 170. [[CrossRef](#)]
60. Ahmed, S.; Rasul, M.G.; Martens, W.N.; Brown, R.; Hashib, M.A. Advances in Heterogeneous Photocatalytic Degradation of Phenols and Dyes in Wastewater: A Review. *Water Air Soil Poll* **2011**, *215*, 3–29. [[CrossRef](#)]
61. Khasawneh, O.F.S.; Palaniandy, P. Photocatalytic Degradation of Pharmaceuticals Using TiO₂ Based Nanocomposite Catalyst-Review. *Civ. Environ. Eng. Rep.* **2019**, *29*, 1–33. [[CrossRef](#)]
62. Rochkind, M.; Pasternak, S.; Paz, Y. Using Dyes for Evaluating Photocatalytic Properties: A Critical Review. *Molecules* **2015**, *20*, 88–110. [[CrossRef](#)] [[PubMed](#)]
63. Raizada, P.; Singh, P.; Kumar, A.; Sharma, G.; Pare, B.; Jonnalagadda, S.B.; Thakur, P. Solar Photocatalytic Activity of Nano-ZnO Supported on Activated Carbon or Brick Grain Particles: Role of Adsorption in Dye Degradation. *Appl. Catal. A Gen.* **2014**, *486*, 159–169. [[CrossRef](#)]
64. Porley, V.; Robertson, N. 6—Substrate and Support Materials for Photocatalysis. In *Micro and Nano Technologies*; Boukherroub, R., Ogale, S.B., Robertson, N.B.T.-N.P., Eds.; Elsevier: Amsterdam, The Netherlands, 2020; pp. 129–171. ISBN 978-0-12-817836-2.
65. Valadez-Renteria, E.; Oliva, J.; Rodriguez-Gonzalez, V. Photocatalytic Materials Immobilized on Recycled Supports and Their Role in the Degradation of Water Contaminants: A Timely Review. *Sci. Total Environ.* **2022**, *807*, 150820. [[CrossRef](#)] [[PubMed](#)]
66. Chen, Y.; Ran, M.; Zhou, Z.; Han, X.; Zhu, H.; Gu, J. Lanthanum/Titanium Dioxide Immobilized onto Industrial Waste with Enhanced Photocatalytic Activity, and the Degradation of Dimethyl Phthalate. *J. Clean Prod.* **2021**, *321*, 129014. [[CrossRef](#)]
67. Li, J.; Yao, L.; Wu, D.; King, J.; Chuang, S.S.C.; Liu, B.; Peng, Z. Electrocatalytic Methane Oxidation to Ethanol on Iron-Nickel Hydroxide Nanosheets. *Appl. Catal. B* **2022**, *316*, 121657. [[CrossRef](#)]
68. Xiong, H.; Kunwar, D.; Jiang, D.; García-Vargas, C.E.; Li, H.; Du, C.; Canning, G.; Pereira-Hernandez, X.I.; Wan, Q.; Lin, S.; et al. Engineering Catalyst Supports to Stabilize PdOx Two-Dimensional Rafts for Water-Tolerant Methane Oxidation. *Nat. Catal.* **2021**, *4*, 830–839. [[CrossRef](#)]
69. Fornaciari, J.C.; Primc, D.; Kawashima, K.; Wygant, B.R.; Verma, S.; Spanu, L.; Mullins, C.B.; Bell, A.T.; Weber, A.Z. A Perspective on the Electrochemical Oxidation of Methane to Methanol in Membrane Electrode Assemblies. *ACS Energy Lett.* **2020**, *5*, 2954–2963. [[CrossRef](#)]
70. Divins, N.J.; Braga, A.; Vendrell, X.; Serrano, I.; Garcia, X.; Soler, L.; Lucentini, I.; Danielis, M.; Mussio, A.; Colussi, S.; et al. Investigation of the Evolution of Pd-Pt Supported on Ceria for Dry and Wet Methane Oxidation. *Nat. Commun.* **2022**, *13*, 5080. [[CrossRef](#)]
71. Zhang, X.; Rabiee, H.; Frank, J.; Cai, C.; Stark, T.; Viridis, B.; Yuan, Z.; Hu, S. Enhancing Methane Oxidation in a Bioelectrochemical Membrane Reactor Using a Soluble Electron Mediator. *Biotechnol. Biofuels* **2020**, *13*, 173. [[CrossRef](#)]
72. Zhang, X.; Yuan, Z.; Hu, S. Anaerobic Oxidation of Methane Mediated by Microbial Extracellular Respiration. *Environ. Microbiol. Rep.* **2021**, *13*, 790–804. [[CrossRef](#)] [[PubMed](#)]

73. Zhang, S. The Opportunities and Challenges of Silica Nanomaterial for Atherosclerosis. *Int. J. Nanomed* **2021**, *16*, 701–714. [[CrossRef](#)]
74. Holz, L.I.V.; Loureiro, F.J.A.; Araújo, A.J.M.; Graça, V.C.D.; Mendes, D.; Mendes, A.; Fagg, D.P. The Electrochemical Promotion of Nitrous Oxide Reduction on a Lanthanum Strontium Iron Cobalt Cathode. *Int. J. Energy Res.* **2022**, 1–11. [[CrossRef](#)]
75. Gómez, R.; Weaver, M.J. Reduction of Nitrous Oxide on Iridium Single-Crystal Electrodes. *Langmuir* **2002**, *18*, 4426–4432. [[CrossRef](#)]
76. Kudo, A.; Mine, A. Electrocatalytic Reduction of Nitrous Oxide on Metal and Oxide Electrodes in Aqueous Solution. *Appl. Surf. Sci.* **1997**, *121–122*, 538–542. [[CrossRef](#)]
77. Hansen, K.K. Electrochemical Reduction of Nitrous Oxide on $\text{La}_{1-x}\text{Sr}_x\text{FeO}_3$ Perovskites. *Mater. Res. Bull.* **2010**, *45*, 1334–1337. [[CrossRef](#)]
78. Deeba, R.; Molton, F.; Chardon-Noblat, S.; Costentin, C. Effective Homogeneous Catalysis of Electrochemical Reduction of Nitrous Oxide to Dinitrogen at Rhenium Carbonyl Catalysts. *ACS Catal.* **2021**, *11*, 6099–6103. [[CrossRef](#)]
79. Chen, S.-M.; Li, S.-H.; Thangamuthu, R. Electrochemical Preparation, Characterization, and Electrocatalytic Properties of OsPtCl_6 Film Electrodes Towards Reduction of NAD^+ , Chloroacetic Acids, and Nitrous Oxide. *Electroanalysis* **2009**, *21*, 1505–1513. [[CrossRef](#)]
80. Valenzuela, E.I.; Padilla-Loma, C.; Gómez-Hernández, N.; López-Lozano, N.E.; Casas-Flores, S.; Cervantes, F.J. Humic Substances Mediate Anaerobic Methane Oxidation Linked to Nitrous Oxide Reduction in Wetland Sediments. *Front. Microbiol.* **2020**, *11*, 1–13. [[CrossRef](#)]
81. Harter, J.; Krause, H.-M.; Schuettler, S.; Ruser, R.; Fromme, M.; Scholten, T.; Kappler, A.; Behrens, S. Linking N_2O Emissions from Biochar-Amended Soil to the Structure and Function of the N-Cycling Microbial Community. *ISME J.* **2014**, *8*, 660–674. [[CrossRef](#)]
82. Bi, S.; Liu, H.; Chen, Y.; Hu, Y. Promoting Interspecies Hydrogen/Electron Transfer in Bio-PdNPs-Mediated Denitrification with the Selectivity towards N_2 . *Biochem. Eng. J.* **2022**, *181*, 108395. [[CrossRef](#)]
83. Zhang, S.; Kong, Z.; Wang, H.; Yan, Q.; Vayenas, D. V Enhanced Nitrate Removal by Biochar Supported Nano Zero-Valent Iron (nZVI) at Biocathode in Bioelectrochemical System (BES). *Chem. Eng. J.* **2022**, *433*, 133535. [[CrossRef](#)]
84. Hauser, I.; Colaço, A.B.; Skjæran, J.A.; Einbu, A.; Østgaard, K.; Svendsen, H.F.; Cervantes, F.J. Biological N Removal from Wastes Generated from Amine-Based CO_2 Capture: Case Monoethanolamine. *Appl. Biochem. Biotech.* **2013**, *169*, 1449–1458. [[CrossRef](#)] [[PubMed](#)]
85. Nithin Mithra, S.; Ahankari, S.S. Nanocellulose-Based Membranes for CO_2 Separation from Biogas through the Facilitated Transport Mechanism: A Review. *Mater. Today Sustain.* **2022**, *19*, 100191. [[CrossRef](#)]
86. De Torquato, L.D.M.; Grattieri, M. Photobioelectrochemistry of Intact Photosynthetic Bacteria: Advances and Future Outlook. *Curr. Opin. Electrochem.* **2022**, *34*, 101018. [[CrossRef](#)]
87. Gacitua, M.; Urrejola, C.; Carrasco, J.; Vicuña, R.; Sraín, B.M.; Pantoja-Gutiérrez, S.; Leech, D.; Antiochia, R.; Tasca, F. Use of a Thermophile Desiccation-Tolerant Cyanobacterial Culture and Os Redox Polymer for the Preparation of Photocurrent Producing Anodes. *Front. Bioeng. Biotechnol.* **2020**, *8*, 900. [[CrossRef](#)]
88. Liu, L.; Choi, S. Enhanced Biophotovoltaic Generation in Cyanobacterial Biophotovoltaics with Intracellularly Biosynthesized Gold Nanoparticles. *J. Power Sources* **2021**, *506*, 230251. [[CrossRef](#)]
89. Goh, P.S.; Ismail, A.F. Nanocomposites for Environmental and Energy Applications. *Nanomaterials* **2021**, *11*, 345. [[CrossRef](#)]
90. Moghaddam, H.K.; Pakizeh, M. Experimental Study on Mercury Ions Removal from Aqueous Solution by MnO_2/CNTs Nanocomposite Adsorbent. *J. Ind. Eng. Chem.* **2015**, *21*, 221–229. [[CrossRef](#)]
91. Qian, X.; Wu, Y.; Kan, M.; Fang, M.; Yue, D.; Zeng, J.; Zhao, Y. FeOOH Quantum Dots Coupled g-C 3N_4 for Visible Light Driving Photo-Fenton Degradation of Organic Pollutants. *Appl. Catal. B* **2018**, *237*, 513–520. [[CrossRef](#)]
92. Ahmad, M.Z.; Bhatti, I.A.; Qureshi, K.; Ahmad, N.; Nisar, J.; Zuber, M.; Ashar, A.; Khan, M.I.; Iqbal, M. Graphene Oxide Supported $\text{Fe}_2(\text{MoO}_4)_3$ Nano Rods Assembled Round-Ball Fabrication via Hydrothermal Route and Photocatalytic Degradation of Nonsteroidal Anti-Inflammatory Drug. *J. Mol. Liq.* **2020**, *301*, 112343. [[CrossRef](#)]
93. Du, C.; Zhang, Z.; Yu, G.; Wu, H.; Chen, H.; Zhou, L.; Zhang, Y.; Su, Y.; Tan, S.; Yang, L.; et al. A Review of Metal Organic Framework (MOFs)-Based Materials for Antibiotics Removal via Adsorption and Photocatalysis. *Chemosphere* **2021**, *272*, 129501. [[CrossRef](#)] [[PubMed](#)]
94. Safari, M.; Rezaee, R.; Soltani, R.D.C.; Asgari, E. Dual Immobilization of Magnetite Nanoparticles and Biosilica within Alginate Matrix for the Adsorption of Cd(II) from Aquatic Phase. *Sci. Rep.* **2022**, *12*, 11473. [[CrossRef](#)] [[PubMed](#)]
95. Zhang, B.; Xu, L.; Zhao, Z.; Peng, S.; Yu, C.; Zhang, X. Enhanced Phosphate Removal by Nano-Lanthanum Hydroxide Embedded Silica Aerogel Composites: Superior Performance and Insights into Specific Adsorption Mechanism. *Sep. Purif. Technol.* **2022**, *285*, 120365. [[CrossRef](#)]
96. Ndolomingo, M.J.; Bingwa, N.; Meijboom, R. Review of Supported Metal Nanoparticles: Synthesis Methodologies, Advantages and Application as Catalysts. *J. Mater. Sci.* **2020**, *55*, 6195–6241. [[CrossRef](#)]
97. Karczmarzka, A.; Adamek, M.; El Houbbadi, S.; Kowalczyk, P.; Laskowska, M. Carbon-Supported Noble-Metal Nanoparticles for Catalytic Applications-A Review. *Crystals* **2022**, *12*, 584. [[CrossRef](#)]
98. Sharma, G.; Sharma, S.; Kumar, A.; Lai, C.W.; Naushad, M.; Iqbal, J.; Stadler, F.J. Activated Carbon as Superadsorbent and Sustainable Material for Diverse Applications. *Adsorpt. Sci. Technol.* **2022**, *2022*, 4184809. [[CrossRef](#)]

99. Ramírez-Montoya, L.A.; Hernández-Montoya, V.; Montes-Morán, M.A. Optimizing the Preparation of Carbonaceous Adsorbents for the Selective Removal of Textile Dyes by Using Taguchi Methodology. *J. Anal. Appl. Pyrolysis* **2014**, *109*, 9–20. [[CrossRef](#)]
100. Delgadillo-Velasco, L.; Hernández-Montoya, V.; Ramírez-Montoya, L.A.; Montes-Morán, M.A.; del Rosario Moreno-Virgen, M.; Rangel-Vázquez, N.A. Removal of Phosphate and Aluminum from Water in Single and Binary Systems Using Iron-Modified Carbons. *J. Mol. Liq.* **2021**, *323*, 114586. [[CrossRef](#)]
101. Liu, J.; Jiang, J.; Meng, Y.; Aihemaiti, A.; Xu, Y.; Xiang, H.; Gao, Y.; Chen, X. Preparation, Environmental Application and Prospect of Biochar-Supported Metal Nanoparticles: A Review. *J. Hazard. Mater.* **2020**, *388*, 122026. [[CrossRef](#)]
102. Jjagwe, J.; Wilberforce, P.; Menya, E.; Mpagi, H. Synthesis and Application of Granular Activated Carbon from Biomass Waste Materials for Water Treatment: A Review. *J. Bioresour. Bioprod.* **2021**, *6*, 292–322. [[CrossRef](#)]
103. Awang, N.A.; Wan Salleh, W.N.; Aziz, F.; Yusof, N.; Ismail, A.F. A Review on Preparation, Surface Enhancement and Adsorption Mechanism of Biochar-Supported Nano Zero-Valent Iron Adsorbent for Hazardous Heavy Metals. *J. Chem. Technol. Biotechnol.* **2022**, 1–23. [[CrossRef](#)]
104. Durán-Jiménez, G.; Stevens, L.A.; Kostas, E.T.; Hernández-Montoya, V.; Robinson, J.P.; Binner, E.R. Rapid, Simple and Sustainable Synthesis of Ultra-Microporous Carbons with High Performance for CO₂ Uptake, via Microwave Heating. *Chem. Eng. J.* **2020**, *388*, 1–13. [[CrossRef](#)]
105. Ho, S.-H.; Zhu, S.; Chang, J.-S. Recent Advances in Nanoscale-Metal Assisted Biochar Derived from Waste Biomass Used for Heavy Metals Removal. *Bioresour. Technol.* **2017**, *246*, 123–134. [[CrossRef](#)]
106. Rodríguez-Narvaez, O.M.; Peralta-Hernandez, J.M.; Goonetilleke, A.; Bandala, E.R. Biochar-Supported Nanomaterials for Environmental Applications. *J. Ind. Eng. Chem.* **2019**, *78*, 21–33. [[CrossRef](#)]
107. Aigbe, U.O.; Ukhurebor, K.E.; Onyancha, R.B.; Okundaye, B.; Pal, K.; Osibote, O.A.; Esiekpe, E.L.; Kusuma, H.S.; Darmokoesomo, H. A Facile Review on the Sorption of Heavy Metals and Dyes Using Bionanocomposites. *Adsorpt. Sci. Technol.* **2022**, *2022*, 8030175. [[CrossRef](#)]
108. Ramírez-Montoya, L.A.; Hernández-Montoya, V.; Bonilla-Petriciolet, A.; Montes-Morán, M.A.; Tovar-Gómez, R.; Moreno-Virgen, M.R. Preparation, Characterization and Analyses of Carbons with Natural and Induced Calcium Compounds for the Adsorption of Fluoride. *J. Anal. Appl. Pyrolysis* **2014**, *105*, 75–82. [[CrossRef](#)]
109. Su, C.; Zhao, L.; Liao, L.; Qin, J.; Lu, Y.; Deng, Q.; Chen, M.; Huang, Z. Application of Biochar in a CIC Reactor to Relieve Ammonia Nitrogen Stress and Promote Microbial Community during Food Waste Treatment. *J. Clean Prod.* **2019**, *209*, 353–362. [[CrossRef](#)]
110. Fallah, Z.; Zare, E.N.; Ghomi, M.; Ahmadijokani, F.; Amini, M.; Tajbakhsh, M.; Arjmand, M.; Sharma, G.; Ali, H.; Ahmad, A.; et al. Toxicity and Remediation of Pharmaceuticals and Pesticides Using Metal Oxides and Carbon Nanomaterials. *Chemosphere* **2021**, *275*, 130055. [[CrossRef](#)]
111. Fei, L.; Bilal, M.; Qamar, S.A.; Imran, H.M.; Riasat, A.; Jahangeer, M.; Ghafoor, M.; Ali, N.; Iqbal, H.M.N. Nano-Remediation Technologies for the Sustainable Mitigation of Persistent Organic Pollutants. *Environ. Res.* **2022**, *211*, 113060. [[CrossRef](#)]
112. Manyangadze, M.; Chikuruwo, N.H.M.; Narsaiah, T.B.; Chakra, C.S.; Radhakumari, M.; Danha, G. Enhancing Adsorption Capacity of Nano-Adsorbents via Surface Modification: A Review. *South Afr. J. Chem. Eng.* **2020**, *31*, 25–32. [[CrossRef](#)]
113. Liu, S.; Zhang, S.; Fan, M.; Yuan, Y.; Sun, X.; Wang, D.; Xu, Y. High-Efficiency Adsorption of Various Heavy Metals by Tea Residue Biochar Loaded with Nanoscale Zero-Valent Iron. *Environ. Prog Sustain.* **2021**, *40*, e13706. [[CrossRef](#)]
114. Bargougui, R.; Bouazizi, N.; Brun, N.; Fotsing, P.N.; Thoumire, O.; Ladam, G.; Woumfo, E.D.; Mofaddel, N.; Le Derf, F.; Vieillard, J. Improvement in CO₂ Adsorption Capacity of Cocoa Shell through Functionalization with Amino Groups and Immobilization of Cobalt Nanoparticles. *J. Environ. Chem. Eng.* **2018**, *6*, 325–331. [[CrossRef](#)]
115. Lu, H.P.; Li, Z.A.; Gascó, G.; Méndez, A.; Shen, Y.; Paz-Ferreiro, J. Use of Magnetic Biochars for the Immobilization of Heavy Metals in a Multi-Contaminated Soil. *Sci. Total Environ.* **2018**, *622–623*, 892–899. [[CrossRef](#)]
116. Liu, Y.; Liu, Z.; Gao, J.; Dai, J.; Han, J.; Wang, Y.; Xie, J.; Yan, Y. Selective Adsorption Behavior of Pb (II) by Mesoporous Silica SBA-15-Supported Pb (II) -Imprinted Polymer Based on Surface Molecularly Imprinting Technique. *J. Hazard. Mater.* **2011**, *186*, 197–205. [[CrossRef](#)] [[PubMed](#)]
117. Guerra, F.D.; Attia, M.F.; Whitehead, D.C.; Alexis, F. Nanotechnology for Environmental Remediation: Materials and Applications. *Molecules* **2018**, *23*, 1760. [[CrossRef](#)] [[PubMed](#)]
118. Su, G.; Zhong, X.; Qiu, S.; Fan, J.; Zhou, H.; Zhou, X. Preparation of Mesoporous Silica-Based Nanocomposites with Synergistically Antibacterial Performance from Nano-Metal (Oxide) and Polydopamine. *Nanotechnology* **2022**, *33*, 155702. [[CrossRef](#)] [[PubMed](#)]
119. Popa, A.; Visa, A.; Maranescu, B.; Hulka, I.; Lupa, L. Chemical Modification of Chitosan for Removal of Pb (II) Ions from Aqueous Solutions. *Materials* **2021**, *14*, 7894. [[CrossRef](#)]
120. Jiang, D.; Chu, B.; Amano, Y.; Machida, M. Removal and Recovery of Phosphate from Water by Mg-Laden Biochar: Batch and Column Studies. *Colloids Surface A* **2018**, *558*, 429–437. [[CrossRef](#)]
121. Dehghani, M.H.; Karri, R.R.; Alimohammadi, M.; Nazmara, S.; Zarei, A.; Saeedi, Z. Insights into Endocrine-Disrupting Bisphenol-A Adsorption from Pharmaceutical Effluent by Chitosan Immobilized Nanoscale Zero-Valent Iron Nanoparticles. *J. Mol. Liq.* **2020**, *311*, 113317. [[CrossRef](#)]
122. Srivastava, V.; Choubey, A.K. Investigation of Adsorption of Organic Dyes Present in Wastewater Using Chitosan Beads Immobilized with Biofabricated CuO Nanoparticles. *J. Mol. Struct.* **2021**, *1242*, 130749. [[CrossRef](#)]

123. Lin, R.; Cheng, J.; Zhang, J.; Zhou, J.; Cen, K.; Murphy, J.D. Boosting Biomethane Yield and Production Rate with Graphene: The Potential of Direct Interspecies Electron Transfer in Anaerobic Digestion. *Bioresour. Technol.* **2017**, *239*, 345–352. [[CrossRef](#)]
124. Bombuwala Dewage, N.; Liyanage, A.S.; Pittman, C.U.; Mohan, D.; Mlsna, T. Fast Nitrate and Fluoride Adsorption and Magnetic Separation from Water on α -Fe₂O₃ and Fe₃O₄ Dispersed on Douglas Fir Biochar. *Bioresour. Technol.* **2018**, *263*, 258–265. [[CrossRef](#)]
125. Yang, F.; Zhang, S.; Sun, Y.; Cheng, K.; Li, J.; Tsang, D.C.W. Fabrication and Characterization of Hydrophilic Corn Stalk Biochar-Supported Nanoscale Zero-Valent Iron Composites for Efficient Metal Removal. *Bioresour. Technol.* **2018**, *265*, 490–497. [[CrossRef](#)] [[PubMed](#)]
126. Ma, X.; Zhao, S.; Tian, Z.; Duan, G.; Pan, H.; Yue, Y. MOFs Meet Wood: Reusable Magnetic Hydrophilic Composites toward Efficient Water Treatment with Super-High Dye Adsorption Capacity at High Dye Concentration. *Chem. Eng. J.* **2022**, *446*, 136851. [[CrossRef](#)]
127. Wang, X.; Zhang, Y.; Shan, R.; Hu, H. Polydopamine Interface Encapsulating Graphene and Immobilizing Ultra-Small, Active Fe₃O₄ Nanoparticles for Organic Dye Adsorption. *Ceram. Int.* **2021**, *47*, 3219–3231. [[CrossRef](#)]
128. Maranescu, B.; Popa, A.; Lupa, L.; Maranescu, V.; Viisa, A. Use of Chitosan Complex with Aminophosphonic Groups and Cobalt for the Removal of Sr²⁺ Ions. *Sep. Sci. Technol.* **2018**, *53*, 1058–1064. [[CrossRef](#)]
129. Di Natale, F.; Gargiulo, V.; Alfè, M. Adsorption of Heavy Metals on Silica-Supported Hydrophilic Carbonaceous Nanoparticles (SHNPs). *J. Hazard. Mater.* **2020**, *393*, 122374. [[CrossRef](#)]
130. Sanghuaypai, P.; Sirikanjanawanit, N.; Sukpirom, N.; Chaianansutcharit, S.; Ngeontae, W.; Imyim, A. Gold Nanoparticles Supported on Functionalized Silica for Adsorption and Oxidation of Toluene. *Mater. Chem. Phys.* **2022**, *281*, 125904. [[CrossRef](#)]
131. Jiang, Z.-J.; Liu, C.-Y.; Sun, L.-W. Catalytic Properties of Silver Nanoparticles Supported on Silica Spheres. *J. Phys. Chem. B* **2005**, *109*, 1730–1735. [[CrossRef](#)]
132. Molina, C.B.; Calvo, L.; Gilarranz, M.A.; Casas, J.A.; Rodriguez, J.J. Pd–Al Pillared Clays as Catalysts for the Hydrodechlorination of 4-Chlorophenol in Aqueous Phase. *J. Hazard. Mater.* **2009**, *172*, 214–223. [[CrossRef](#)] [[PubMed](#)]
133. Gurav, J.L.; Jung, I.-K.; Park, H.-H.; Kang, E.S.; Nadargi, D.Y. Silica Aerogel: Synthesis and Applications. *J. Nanomater.* **2010**, *2010*, 409310. [[CrossRef](#)]
134. Peng, X.; Cheng, K.; Kang, J.; Gu, B.; Yu, X.; Zhang, Q.; Wang, Y. Impact of Hydrogenolysis on the Selectivity of the Fischer–Tropsch Synthesis: Diesel Fuel Production over Mesoporous Zeolite-Y-Supported Cobalt Nanoparticles. *Angew Chem. Int. Edit.* **2015**, *54*, 4553–4556. [[CrossRef](#)] [[PubMed](#)]
135. Cheng, D.; Jin, W.; Zhan, X.; Chen, F. Alumina Membrane Coated Activated Carbon: A Novel Strategy to Enhance the Mechanical Properties of a Solid Catalyst. *RSC Adv.* **2016**, *6*, 10229–10232. [[CrossRef](#)]
136. Li, C.M.; Wang, X.P.; Jiao, Z.H.; Zhang, Y.S.; Yin, X.B.; Cui, X.M.; Wei, Y.Z. Functionalized Porous Silica-Based Nano/Micro Particles for Environmental Remediation of Hazard Ions. *Nanomaterials* **2019**, *9*, 247. [[CrossRef](#)]
137. Li, X.; Ai, S.; Huang, Y.; Huang, C.; Yu, W.; Mao, Z. Fast and Reversible Adsorption for Dibenzothiophene in Fuel Oils with Metallic Nano-Copper Supported on Mesoporous Silica. *Environ. Sci. Pollut. R* **2021**, *28*, 2741–2752. [[CrossRef](#)]
138. Garg, R.; Garg, R.; Okon Eddy, N.; Ibrahim Almohana, A.; Fahad Almojil, S.; Amir Khan, M.; Ho Hong, S. Biosynthesized Silica-Based Zinc Oxide Nanocomposites for the Sequestration of Heavy Metal Ions from Aqueous Solutions. *J. King Saud Univ. Sci.* **2022**, *34*, 101996. [[CrossRef](#)]
139. Avella, M.; Buzarovska, A.; Errico, M.E.; Gentile, G.; Grozdanov, A. Eco-Challenges of Bio-Based Polymer Composites. *Materials* **2009**, *2*, 911–925. [[CrossRef](#)]
140. Zhao, X.; Lv, L.; Pan, B.; Zhang, W.; Zhang, S.; Zhang, Q. Polymer-Supported Nanocomposites for Environmental Application: A Review. *Chem. Eng. J.* **2011**, *170*, 381–394. [[CrossRef](#)]
141. Ambroggi, V.; Pietrella, D.; Donnadio, A.; Latterini, L.; Di Michele, A.; Luffarelli, I.; Ricci, M. Biocompatible Alginate Silica Supported Silver Nanoparticles Composite Films for Wound Dressing with Antibiofilm Activity. *Mater Sci. Eng: C* **2020**, *112*, 110863. [[CrossRef](#)]
142. Yang, Z.; Si, S.; Zhang, C. Magnetic Single-Enzyme Nanoparticles with High Activity and Stability. *Biochem. Biophys. Res. Commun.* **2008**, *367*, 169–175. [[CrossRef](#)] [[PubMed](#)]
143. Mallón, L.; Cerezo-Navarrete, C.; Romero, N.; Puche, M.; García-Antón, J.; Bofill, R.; Philippot, K.; Martínez-Prieto, L.M.; Sala, X. Ru Nanoparticles Supported on Alginate-Derived Graphene as Hybrid Electrodes for the Hydrogen Evolution Reaction. *New J. Chem.* **2022**, *46*, 49–56. [[CrossRef](#)]
144. Qian, H.; Wang, J.; Yan, L. Synthesis of Lignin-Poly (N-Methylaniline) -Reduced Graphene Oxide Hydrogel for Organic Dye and Lead Ions Removal. *J. Bioresour. Bioprod.* **2020**, *5*, 204–210. [[CrossRef](#)]
145. Sierra-Martin, B.; Fernandez-Barbero, A. Inorganic/Polymer Hybrid Nanoparticles for Sensing Applications. *Adv. Colloid Interfac.* **2016**, *233*, 25–37. [[CrossRef](#)] [[PubMed](#)]
146. Ali, H.S.H.M.; Khan, S.A. Stabilization of Various Zero-Valent Metal Nanoparticles on a Superabsorbent Polymer for the Removal of Dyes, Nitrophenol, and Pathogenic Bacteria. *ACS Omega* **2020**, *5*, 7379–7391. [[CrossRef](#)]
147. Song, Y.; Zeng, Y.; Liao, J.; Chen, J.; Du, Q. Chemosphere Efficient Removal of Sulfamethoxazole by Resin-Supported Zero-Valent Iron Composites with Tunable Structure: Performance, Mechanisms, and Degradation Pathways. *Chemosphere* **2021**, *269*, 128684. [[CrossRef](#)]
148. Mohammadnezhad, G.; Keikavousi, A. Polymer Matrix Nanocomposites for Heavy Metal Adsorption: A Review. *J. Iran. Chem. Soc.* **2020**, *17*, 1259–1281. [[CrossRef](#)]

149. Su, Q.; Pan, B.; Pan, B.; Zhang, Q.; Zhang, W.; Lv, L.; Wang, X.; Wu, J.; Zhang, Q. Fabrication of Polymer-Supported Nanosized Hydrous Manganese Dioxide (HMO) for Enhanced Lead Removal from Waters. *Sci. Total Environ.* **2009**, *407*, 5471–5477. [[CrossRef](#)]
150. Maranescu, B.; Lupa, L.; Visa, A. Synthesis, Characterizations and Pb(II) Sorption Properties of Cobalt Phosphonate. *Materials* **2016**, *88*, 979–992. [[CrossRef](#)]
151. Li, G.; Zhao, S.; Zhang, Y.; Tang, Z. Metal–Organic Frameworks Encapsulating Active Nanoparticles as Emerging Composites for Catalysis: Recent Progress and Perspectives. *Adv. Mater.* **2018**, *30*, 1800702. [[CrossRef](#)] [[PubMed](#)]